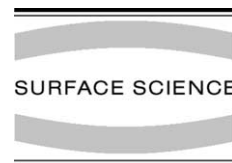




ELSEVIER

Surface Science 504 (2002) 159–166



www.elsevier.com/locate/susc

# Initial stages of praseodymium oxide film formation on Si(001)

H.-J. Müssig<sup>a,\*</sup>, J. Dąbrowski<sup>a</sup>, K. Ignatovich<sup>a,b</sup>, J.P. Liu<sup>a</sup>, V. Zavodinsky<sup>a,b</sup>,  
H.J. Osten<sup>a</sup>

<sup>a</sup> IHP, Im Technologiepark 25, D-15236 Frankfurt (Oder), Germany

<sup>b</sup> IACP FEB RAN, Radio 5, 69041 Vladivostok, Russia

Received 8 September 2001; accepted for publication 3 December 2001

## Abstract

Pr<sub>2</sub>O<sub>3</sub> may be an alternative high-*K* gate dielectric material for silicon integrated circuits, i.e., it has a dielectric constant  $K \geq 25$  and is currently under consideration as potential replacement for SiO<sub>2</sub> as the gate dielectric material for sub-0.1 μm complementary metal-oxide-semiconductor technology. Using scanning tunneling microscopy and X-ray photoelectron spectroscopy, we show that the initial stages of heteroepitaxial Pr<sub>2</sub>O<sub>3</sub> grown on Si(001) consist of a mixed PrO<sub>2</sub>/Pr<sub>2</sub>O<sub>3</sub> phase. First ab initio calculation results also indicate the formation of an ultra-thin Si–O interlayer between the Si substrate and Pr<sub>2</sub>O<sub>3</sub>. In the monolayer range of deposited Pr<sub>2</sub>O<sub>3</sub>, Auger electron spectroscopy measurements show that the oxide is completely decomposed above 780 °C. © 2002 Elsevier Science B.V. All rights reserved.

**Keywords:** Growth; Scanning tunneling microscopy; X-ray photoelectron spectroscopy; Auger electron spectroscopy; Silicon; Ab initio quantum chemical methods and calculations

## 1. Introduction

Crystalline praseodymium oxide in the form of Pr<sub>2</sub>O<sub>3</sub> on silicon is a promising high-*K* dielectric with an effective dielectric constant of around 30 and very low leakage currents [1]. Here, we report on the initial stages of heteroepitaxial growth on Si(001) in two orthogonal in-plane directions studied by scanning tunneling microscopy (STM). We present experimental evidence and theoretical explanation based on X-ray photoelectron spectro-

scopy (XPS) measurements and ab initio pseudo-potential simulations for the transition of PrO<sub>2</sub> into Pr<sub>2</sub>O<sub>3</sub>, and the formation of an ultra-thin Si–O interlayer between Pr<sub>2</sub>O<sub>3</sub> and the Si substrate. Our results show that in the monolayer range of deposited praseodymium oxide, the thermal stability of such thin films is lower than that of SiO<sub>2</sub>.

Device miniaturization has been the primary means by which the semiconductor industry has achieved the unprecedented gains in productivity and performance. Further scaling implies that silicon-based devices will reach the physical limits of miniaturization within the next 10 years [2,3]. In spite of outstanding properties of SiO<sub>2</sub>, which include high resistivity, excellent dielectric strength, a large band gap, a high melting point, and a native,

\* Corresponding author. Tel.: +49-335-5625700; fax: +49-335-5625327.

E-mail address: muessig@ihp-microelectronics.com (H.-J. Müssig).

low defect density interface with Si [3], SiO<sub>2</sub> suffers from a relatively low dielectric constant  $K = 3.9$ . Since high gate dielectric capacitance is necessary to produce the required drive currents for submission devices [4,5], and further since capacitance is inversely proportional to gate dielectric thickness, the SiO<sub>2</sub> layers have of necessity been scaled to ever thinner dimensions. Under laboratory conditions, it is already possible to produce metal-oxide-semiconductor field-effect transistors (MOSFETs) with a SiO<sub>2</sub> gate oxide thickness of less than 10 atoms [6]. As the SiO<sub>2</sub> thickness is reduced, new technological problems arise. These include the dielectric thickness variation, penetration of impurities from the gate into the gate dielectric, and the reliability and lifetimes of devices made with these ultrathin films [3]. However, the major contributor leading to the limited extendibility of SiO<sub>2</sub> as extremely thin gate dielectric is the exponential increase in gate leakage current with decreasing film thickness.

In the course of SiO<sub>2</sub> oxide thickness reduction, the physical limits are fundamental, i.e., they cannot be overcome by technological improvements. Limiting factors are the interface roughness on atomic scale, and the fact that a monolayer consisting of silicon and oxygen atoms does not have the same atomic arrangement as SiO<sub>2</sub> which, however, is needed to reproduce the local electronic structure of the compact SiO<sub>2</sub>. The challenge is, therefore, to reduce the leakage current while maintaining the same gate capacitance by replacing the traditional SiO<sub>2</sub> gate dielectric by a thicker film of new materials with higher dielectric constant  $K$ .

Our work was motivated by the need for an alternative silicon compatible gate dielectric material with high dielectric constant. We have characterized structurally the initial stages of deposited high- $K$  material on Si(001) in order to understand the influence of a possible thin SiO<sub>2</sub> buffer layer between the Si substrate and the high- $K$  material, and to study the thermal stability for integration into a complementary metal-oxide-semiconductor (CMOS) process.

This paper contains the experimental evidence for heteroepitaxial growth of Pr<sub>2</sub>O<sub>3</sub> on Si(001) and the thermal stability of such thin layers.

In combination with first-principles total-energy calculations, the results indicate that the bond/nuclear charge mismatch at the heterovalent Si-dielectric interface is reduced by forming an ultrathin SiO<sub>x</sub> layer.

## 2. Results and discussion

### 2.1. Experimental

The STM experiments were performed in a ultra-high vacuum (UHV) system from OMI-CRON with several surface analysis facilities and a base pressure in the low 10<sup>-11</sup> mbar range. This system is equipped with a preparation chamber in which cleaning of Si(001) by heat treatment and deposition of praseodymium oxide by e-beam evaporators are possible under the same vacuum conditions as in the analytical chamber.

An undoped, 5000 Ω cm Si(001) wafer with an actual vicinal angle of <0.5° was used for our STM studies. After chemical etching and introducing the sample into the preparation chamber, it was thoroughly outgassed over several hours by indirect current heating at 500 °C. Then, the clean Si(001)(2 × 1) reconstructed surface was prepared by direct heating briefly to 1250 °C, cooling down quickly to about 900 °C and slowly at rates of <2 K/s from 900 °C to room temperature [7]. During the cleaning procedure, the pressure remained in the 10<sup>-10</sup> mbar range.

Pr<sub>6</sub>O<sub>11</sub> was vaporized from a molybdenum crucible by electron bombardment. After degassing of the crucible including Pr<sub>6</sub>O<sub>11</sub> for several hours, Pr<sub>2</sub>O<sub>3</sub> can be deposited on the sample surface at an oxygen residual partial pressure of 5 × 10<sup>-8</sup> mbar. Due to the supersaturation of oxygen at the beginning of evaporation also PrO<sub>2</sub> can be deposited. The Pr<sub>2</sub>O<sub>3</sub> cubic phase is the most stable one, however, it has a relatively large lattice mismatch to Si(001), namely 2.8%, while the PrO<sub>2</sub> fluorite phase has a mismatch only of -1% [8]. That could be a reason why the PrO<sub>2</sub> fluorite phase is preferred to growth heteroepitaxially on Si(001) from the beginning of praseodymium oxide deposition. Usually, the sample temperature was 600 °C.

The geometric, electronic, and chemical structure of the initial stages of praseodymium oxide growth were analyzed by scanning tunneling microscopy (STM), X-ray photoelectron spectroscopy (XPS), and Auger electron spectroscopy (AES).

## 2.2. Heteroepitaxial growth

Fig. 1 shows a series of empty state STM images illustrating the structural changes on Si(001) due to praseodymium oxide deposition. Starting from the  $(2 \times 1)$  reconstructed clean surface (Fig. 1a) with their characteristic dimer rows and monatomic steps, we observe chains of “ad-dimers” oriented vertically to the dimer rows of the clean surface by exposure to praseodymium oxide at 15 nA flux for 1 min and 600 °C (Fig. 1b). If we elongate the exposure time (Fig. 1c) two orthogonally oriented ad-dimer layers can be already recognized. There is a heteroepitaxial growth of praseodymium oxide on Si(001) from the beginning. Although one cannot carry out any chemical analysis by means of STM, we are sure that our later discussed experimental results concerning the XPS measurements and the thermal stability of very thin adsorbate layers indicate clearly that the material adsorbed must be praseodymium oxide.

More detailed investigations of the STM images yield that ad-dimer rows have exactly the  $\times 2$  periodicity of the substrate (Fig. 2). By higher exposure, a  $(3 \times 1)$  periodicity starts to develop. Very small areas of this structure are visible in Fig. 3.

In Fig. 4, the STM image of unoccupied states measured after praseodymium oxide deposition of 10 nA flux for 1 min at 700 °C, i.e., at a substrate temperature elevated by 100 K, shows the transi-

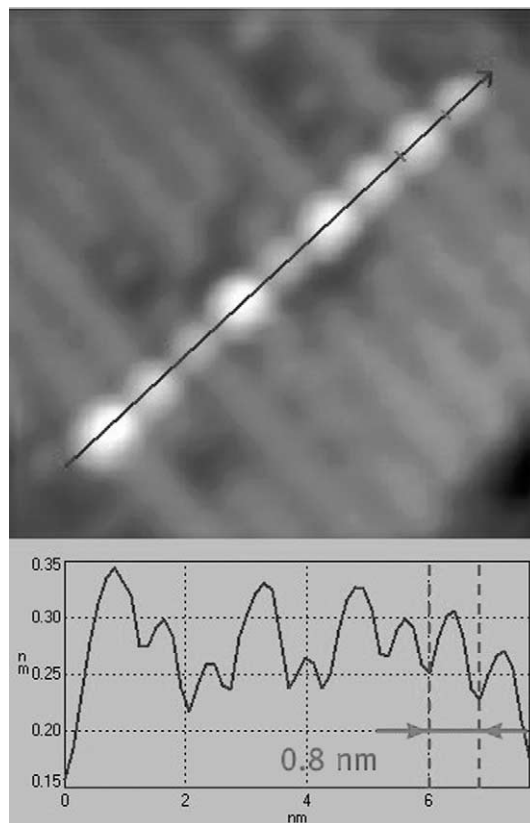


Fig. 2. Detail of Fig. 1b. The ad-dimer row shows the  $\times 2$  periodicity of the substrate.

tion state from ad-dimer rows to the  $(3 \times 1)$  periodicity.

In summary, we found that praseodymium oxide grows on Si(001) in two orthogonal in-plane directions. Deposited molecules diffusing on the surface use dimer rows as convenient “rails”. At a surface temperature of 600 °C, the migration

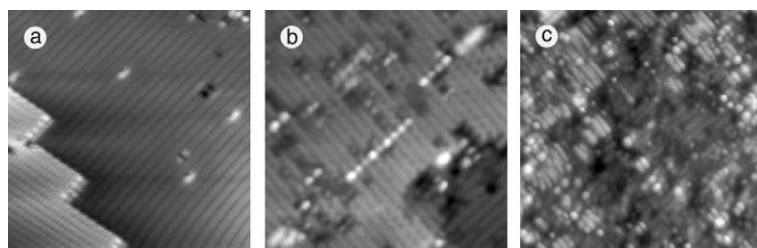


Fig. 1. Empty state STM images ( $20 \times 20 \text{ nm}^2$ ) of (a) the clean reconstructed Si(001)( $2 \times 1$ ) surface, and after praseodymium oxide deposition at 600 °C: (b) 15 nA flux for 1 min, (c) 15 nA flux for 3 min.

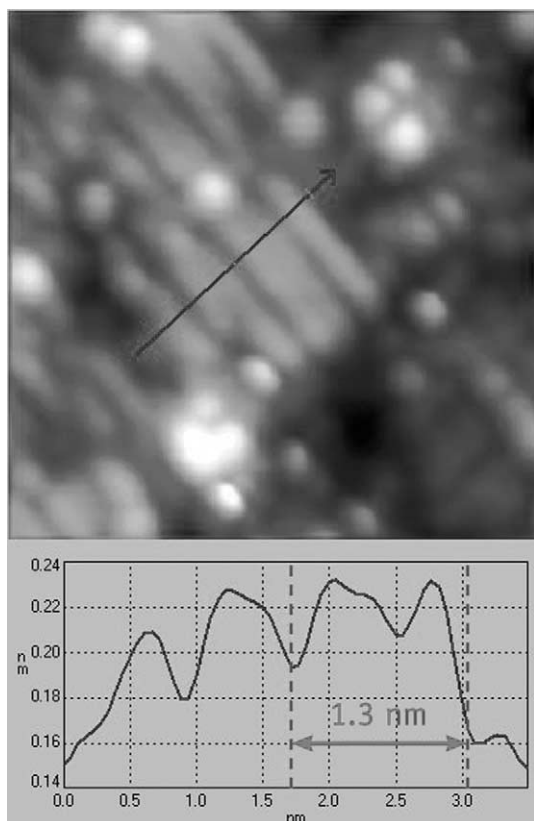


Fig. 3. Detail of Fig. 1c. The line scan indicates that a  $(3 \times 1)$  periodicity develops.

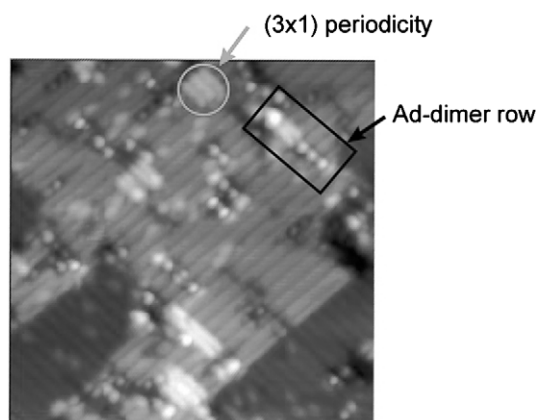


Fig. 4. Empty state STM image of a praseodymium oxide covered Si(001) surface (10 nA flux for 1 min at 700 °C). The transition from ad-dimer rows to the  $(3 \times 1)$  periodicity is clearly visible.

of ad-dimers dominates so that ad-dimer rows are visible.

### 2.3. $\text{Pr}_2\text{O}_3/\text{Si}(001)$ interface formation

We have studied the chemical composition of deposited praseodymium oxide layers on Si(001) using XPS. These experiments were performed in an apparatus for molecular beam epitaxy (MBE) equipped with e-beam evaporators and an XPS system. During praseodymium oxide deposition, the pressure in the MBE growth chamber was similar to that of the STM chamber. Fig. 5a shows the Pr  $3d_{5/2}$  peak intensities as a function of binding energy for eight different oxide layer thicknesses. The thickness of the oxide films was determined by grazing incidence X-ray reflectometry [9], i.e., an X-ray beam at grazing incidence is reflected off of both the film and substrate interfaces producing an interference pattern. The interference pattern immediately yields the thickness of the film. Starting with a thickness of 0.34 nm, we find a shift of the  $3d_{5/2}$  peak to lower energy values with increasing layer thickness to 8.7 nm. Fig. 5b shows the extracted binding energies as a function of layer thickness. We interpret this as a change of the chemical composition from an oxygen-rich praseodymium oxide phase to  $\text{Pr}_2\text{O}_3$  [10].

We now present a simple justification of this interpretation. Because of relatively high oxygen partial pressure of  $5 \times 10^{-8}$  mbar due to the evaporation of  $\text{Pr}_6\text{O}_{11}$ , and because of the small mismatch between the lattice constant of  $\text{PrO}_2$  and the distance between Si(001) atoms, the deposited praseodymium oxide consists initially of  $\text{PrO}_2$  islands (Fig. 6a, left). The stress in such an island is then minimal. Transformation of a thin  $\text{PrO}_2$  island to  $\text{Pr}_2\text{O}_3$  (Fig. 6a, right) would increase the stress if performed without relaxation of the oxide. In principle, a  $\text{Pr}_2\text{O}_3$  island could relax when an amorphous  $\text{SiO}_x$  layer is formed at the interface. However, there exists a critical amount of oxygen needed to amorphize the interface to the extent that it may act as a stress buffer. When the praseodymium oxide layer is thick enough, this oxygen is released from  $\text{PrO}_2$  as it transforms into  $\text{Pr}_2\text{O}_3$ :

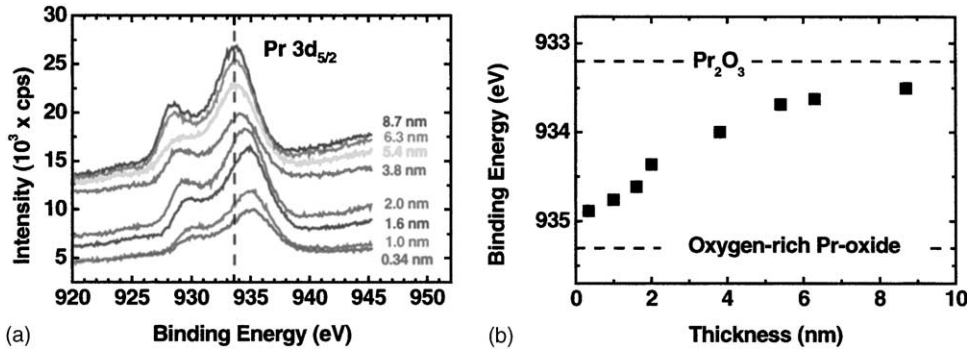


Fig. 5. Pr 3d<sub>5/2</sub> XPS spectra of MBE-grown praseodymium oxide with different thickness. The sample was transferred after growth in vacuo into the XPS chamber. (b) With decreasing film thickness, a shift of the main peak position to higher energies is provable.

Lattice constant PrO <sub>2</sub>		Lattice constant Pr <sub>2</sub> O <sub>3</sub>		Si-Si distance on Si(001)	
Experiment	Calculation	Experiment	Calculation	Experiment	Calculation
0.380 nm	0.372 nm	0.395 nm	0.387 nm	0.384 nm	0.379 nm

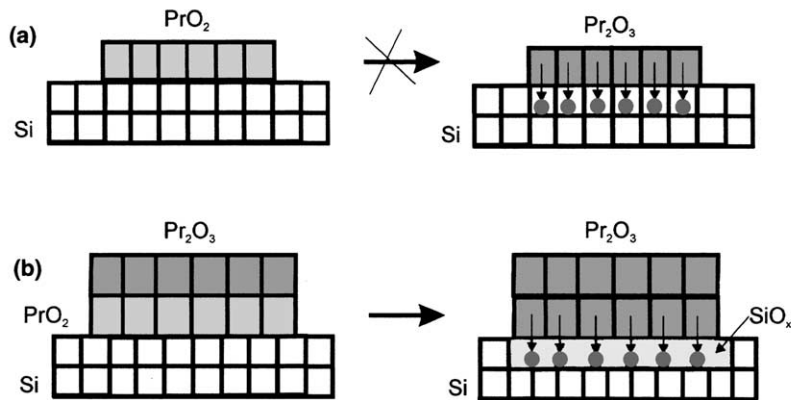
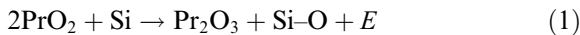


Fig. 6. Model for the transformation of an oxygen-rich praseodymium oxide phase to Pr<sub>2</sub>O<sub>3</sub> (see text). The praseodymium oxide lattice parameters are taken from [8].



where  $E$  is the energy balance of this transformation. In other words, the thickness of the PrO<sub>2</sub> island should be large enough (Fig. 6b, left) so that either it can release enough oxygen to form a sufficiently thick, amorphized SiO<sub>x</sub> interlayer between the Si substrate and the Pr<sub>2</sub>O<sub>3</sub> oxide (Fig. 6b, right), or the reaction has been running for a sufficiently long time for the excess oxygen from the vapor to make such an interfacial layer.

We have verified this model by ab initio calculations for strained and unstrained praseodymium oxide bulk crystals. We note that no real interface between the oxide and the silicon was included in these calculations; their sole purpose was to check whether the assumption of an unstressed PrO<sub>2</sub> layer is plausible at all. We computed the reaction energy  $E$  defined by Eq. (1) for two cases. First, PrO<sub>2</sub> and Pr<sub>2</sub>O<sub>3</sub> crystals were strained to match the Si(001) surface. This provides information on the energetics of epitaxial growth of thin PrO<sub>2</sub> and

its subsequent transformation to  $\text{Pr}_2\text{O}_3$  without relaxation of the praseodymium oxide (Fig. 6a). Second, the  $\text{PrO}_2$  crystal was strained to match the bulk  $\text{Pr}_2\text{O}_3$ . This provides information on the energetics of simultaneous transformation and relaxation of the grown film (Fig. 6b).

The calculations were done by the ab initio pseudopotential plane wave code fhi96md [11] extended by us for atoms with  $f$  type valence electrons. We applied the local density approximation (LDA) for the exchange and correlation energy [12,13] and nonlocal pseudopotentials in the Troullier–Martins scheme [14,15] with 40 Ry cutoff for plane waves and with two special  $k$ -points:  $(1/4, 1/4, 1/4)$  and  $(1/4, 1/4, 3/4)$ . Because of the open  $f$ -shell of Pr atoms, the key problem in such calculations is in construction of the Pr pseudopotential. The first pseudopotential study of praseodymium oxides were reported in [16, 17] where the electronic structures of  $\text{PrO}_2$  and  $\text{Pr}_2\text{O}_3$  have been calculated. It was found that different Pr pseudopotentials are needed for these two oxides. The reason is a different number of  $f$  electrons localized in the ionic core. A pseudopotential with two core  $f$  electrons was constructed for  $\text{Pr}_2\text{O}_3$  (+3 ionic charge), while for  $\text{PrO}_2$  (+4 ionic charge) a core with only one  $f$  electron was used. In this paper, we used the same approach to construct Pr pseudopotentials.

The scheme of calculations was as follows. We compared for the sums of total energies for two systems, namely (i) bulk  $\text{Pr}_2\text{O}_3$  + bulk Si and (ii) bulk  $\text{Pr}_2\text{O}_3$  + bulk Si with embedded oxygen (left- and right-hand sides of Eq. (1)). We did it for three cases. First,  $\text{PrO}_2$  and  $\text{Pr}_2\text{O}_3$  were strained to match the Si(001) surface (compare Fig. 6a, where strained  $\text{PrO}_2$  island is shown). In this way, epitaxial growth of thin  $\text{PrO}_2$  was modeled under assumption that its transformation to  $\text{Pr}_2\text{O}_3$  occurs without stress relaxation. The energy of (i) is lower by 1.2 eV per oxygen atom than the energy of (ii). In other words, reaction (1) is endothermic with the reaction energy  $E = 1.2$  eV. This means that a thin  $\text{PrO}_2$  layer on Si(001) is stable with respect to transformation into thin  $\text{Pr}_2\text{O}_3$  accompanied by oxidation of the silicon substrate.

Second, the lattice spacings of the praseodymium oxides before and after the transformation

were set to that of relaxed  $\text{Pr}_2\text{O}_3$  (Fig. 6b). This assumes that a thin amorphous  $\text{SiO}_x$  layer has been already formed, and that the  $\text{PrO}_2$  film is strained to match the hard  $\text{Pr}_2\text{O}_3$  layer growing on top of the praseodymium oxide. The system (ii) becomes now more stable than (i) by 0.7 eV per oxygen atom: reaction (1) is exothermic, with the reaction energy  $E = -0.7$  eV. Thus, a  $\text{PrO}_2$  layer is unstable when placed between  $\text{Pr}_2\text{O}_3$  and  $\text{SiO}_x$ . As a consequence,  $\text{PrO}_2$  is transformed into  $\text{Pr}_2\text{O}_3$  by oxidation of the silicon substrate.

Third, we considered the case when the transformation begins with the absence of the buffer  $\text{SiO}_x$  layer. The  $\text{PrO}_2$  film (still modeled as a bulk crystal) is then strained before the reaction (system i) and the  $\text{Pr}_2\text{O}_3$  is unstrained after the reaction (system ii). In this case, reaction (1) is still exothermic, with the reaction energy  $E = -0.2$  eV. This means that the need to build a  $\text{SiO}_x$  buffer (which must be present to relax the  $\text{PrO}_2/\text{Si}$  layer and to allow further evolution of the film to the low energy state of  $\text{Pr}_2\text{O}_3/\text{PrO}_2/\text{SiO}_x/\text{Si}$ ) does not impose an additional energy barrier on the reaction (1). Such a barrier might appear if the transition from  $\text{PrO}_2$  strained to match the substrate (the initial state of small, strained islands) to unstrained  $\text{Pr}_2\text{O}_3$  (the final state of a thick, relaxed film attached to the substrate through the buffer layer) would be associated with an energy loss.

#### 2.4. Thermal stability of praseodymium oxide on Si(001)

The thermal stability of very thin praseodymium oxide layers with thicknesses in the monolayer range was studied by AES. Fig. 7 shows the oxygen coverage as a function of temperature. The decomposition of praseodymium oxide and the desorption of SiO begins at 700 °C. At 780 °C, this process is completed. We notice that the thermal stability of very thin praseodymium oxide layers is about 100 K lower in comparison with corresponding  $\text{SiO}_2$  layers.

The question immediately arises: “What happens with the Pr atoms?” Fig. 8a shows an empty state STM image of a Si(001) surface initially covered by  $\text{Pr}_2\text{O}_3$  and subsequently flashed to 1250 °C in order to remove the deposited film. Features typ-

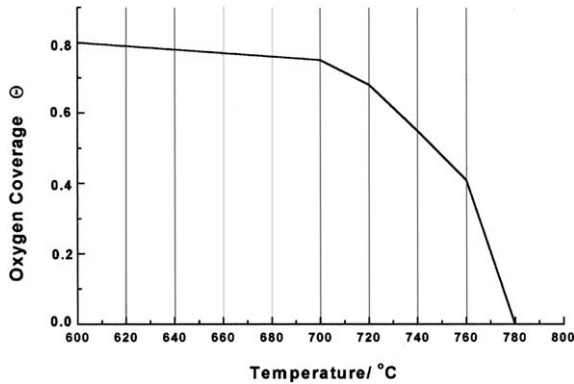


Fig. 7. Thermal stability of a very thin praseodymium oxide layer.

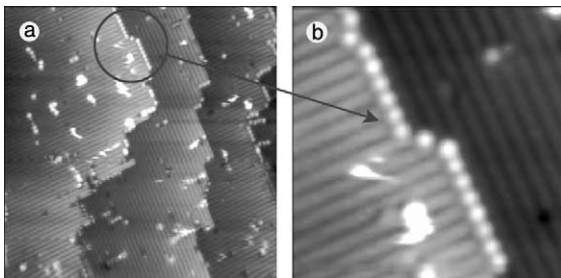


Fig. 8. Empty state STM image after flashing the praseodymium oxide covered surface at 1250 °C: (a)  $50 \times 50 \text{ nm}^2$ , (b) detail. Oxygen desorbs in form of SiO. Pr atoms remain on the surface and migrate to monatomic  $S_B$ -steps. The bright spots represent Pr atoms bonded-in on top positions.

ical for the clean, two-domain Si(001) can be readily recognized: there are dimer rows with orientation changing by  $90^\circ$  at each monatomic step. But in addition to that, numerous bright spots are visible at so-called  $S_B$  steps, i.e., at steps to which the dimer rows run perpendicularly. These bright spots have the periodicity of the dimer rows and are located exactly between them, as visible in Fig. 8b. We interpret this result as follows. After thermal dissociation of  $\text{Pr}_2\text{O}_3$  and desorption of SiO, Pr atoms remaining on the surface diffuse along the dimer rows to  $S_B$  steps, react with Si edge atoms, and form “silicide” manifesting itself as the bright spots. Nevertheless, the physical mechanism responsible for this behavior remains unknown, as are any details of the atomic configuration around Pr atoms adsorbed at step edges.

The thermal stability of small praseodymium oxide coverages was estimated theoretically in the framework of the following model. For low temperatures, i.e., at temperatures at which no Si ad-atoms are present on Si(001), the oxide molecule was assumed to acquire the configuration shown in Fig. 9a. The Pr atom is bonded to four Si atoms via four O atoms. The rest of the surface was assumed to consist of usual Si(001)( $2 \times 1$ ) dimer rows. Total energy  $E_1$  of this system was calculated. Next, we removed the O atoms from the Pr–O–Si bonds and placed them on the Si surface in

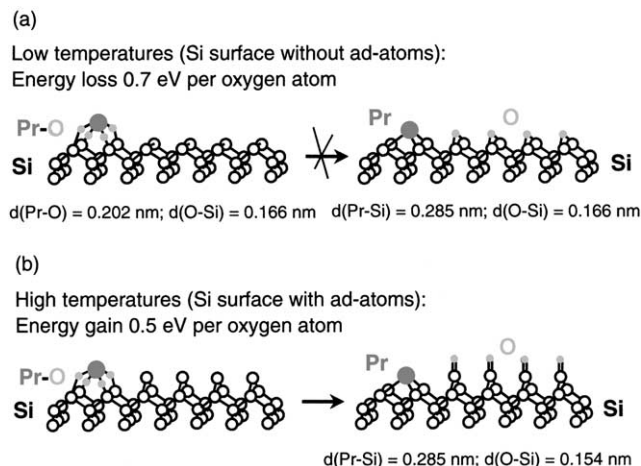


Fig. 9. Ball-and-stick model of the thermal dissociation of praseodymium oxide on Si(001). Pr atoms are drawn as big black circles and O atoms as small gray circles. The atomic distances  $d$  between Pr–O, Pr–Si, and O–Si were calculated.

Si–Si dimer bonds. The Pr atom was then bonded directly to four Si atoms. This increases the energy to  $E_2 = E_1 + E_{\text{SiOSi}}$ , where  $E_{\text{SiOSi}} = 0.7$  eV per O atom compared with the previous one.<sup>1</sup> Therefore, the Pr–O–Si bonds on Si(001) are expected to be stable at low temperatures (e.g., at room temperature). However, when the oxygen atoms were moved not to dimer bonds but to Si ad-atoms (Fig. 9b), the Pr–O bonds became unstable. The total energy of this system was lower by  $E_{\text{SiO}} = -0.5$  eV per O atom than the total energy of the system composed of the oxidized molecule and an unoxidized Si ad-atom.<sup>1</sup> This means that in the presence of Si ad-atoms, praseodymium oxide is expected to dissociate, with the Pr atom forming bonds to Si surface atoms and the O atoms forming silanone (SiO) molecules which can easily desorb from the surface.

### 3. Summary and conclusions

Summarizing, we make the following conclusions.

- STM images show that epitaxial growth of  $\text{Pr}_2\text{O}_3$  on Si(001) in two orthogonal directions begins at early stages.
- The results of XPS measurements and ab initio calculations indicate that an oxygen-rich  $\text{PrO}_2/\text{Pr}_2\text{O}_3$  interlayer is formed between  $\text{Pr}_2\text{O}_3$  and the substrate.
- Ab initio calculations indicate that the  $\text{SiO}_x$  interlayer acts as a buffer compensating the mismatch of atomic distances in the  $\text{Pr}_2\text{O}_3$  film and on the Si(001) substrate.
- Extremely thin praseodymium oxide layers have a lower thermal stability than  $\text{SiO}_2$  layers.
- Pr atoms cannot be removed from the Si(001) surface even by flashing to 1250 °C.

### Acknowledgements

We are very grateful to Abbas Ourmazd for reading the manuscript and critical comments.

### References

- [1] H.J. Osten, J.P. Liu, P. Gaworzewski, E. Bugiel, P. Zaumseil, IEDM Technical Digest (2000) 653.
- [2] International Technology Roadmap for Semiconductors, 1998 update.
- [3] J. Dąbrowski, H.-J. Müssig, Silicon Surfaces and Formation of Interfaces, World Scientific Publishing, Singapore, 2000.
- [4] L. Feldman, E.P. Gusev, E. Garfunkel, in: E. Garfunkel, E.P. Gusev, A.Y. Vul' (Eds.), Fundamental Aspects of Ultrathin Dielectrics on Si-based Devices, Kluwer, Dordrecht, 1998, p. 1.
- [5] G. Timp, R.E. Howard, P.M. Mankiewich, in: G. Timp (Ed.), Nanotechnology, Springer-Verlag, New York, 1998, p. 7.
- [6] H.S. Momose, M. Ono, T. Yoshitomi, T. Ohguro, S. Nakamura, M. Saito, H. Iwai, IEDM Technical Digest (1994) 593.
- [7] B.S. Swartzentruber, Y.-W. Mo, M.B. Webb, M.G. Lagally, J. Vac. Sci. Technol. A 7 (1989) 2901.
- [8] P. Villars, L.D. Calvert, Pearson's Handbook of Crystallographic Data for Intermetallic Phases, 2nd edition, ASM International, Materials Park, Ohio, USA, 1991.
- [9] T.C. Huang, P.C. Cohen, D.J. Eaglesham (Eds.), Advances in Surface and Thin Film Diffraction, Materials Research Society, Warrendale, 1991.
- [10] J.F. Moulder, W.F. Stickle, P.E. Sobol, K.D. Bomben, in: J. Chastain (Ed.), Handbook of X-ray Photoelectron Spectroscopy, Perkin-Elmer Corporation, Eden Prairie, USA, 1992, p. 145.
- [11] M. Bockstedte, A. Kley, J. Neugebauer, M. Scheffler, Comp. Phys. Commun. 107 (1997) 187.
- [12] D.M. Ceperley, B.J. Alder, Phys. Rev. Lett. 45 (1980) 567.
- [13] J.P. Perdew, A. Zunger, Phys. Rev. B 23 (1981) 5048.
- [14] L. Kleinman, D.M. Bylander, Phys. Rev. Lett. 48 (1982) 1425.
- [15] N. Troullier, J.L. Martins, Phys. Rev. B 42 (1991) 1993.
- [16] J. Dąbrowski, V. Zavodinsky, 11th Workshop on Dielectrics in Microelectronics (WODIM 2000), Munich, Germany, Book of Abstracts, 96.
- [17] V. Zavodinsky, J. Dąbrowski, H.-J. Müssig, K. Ignatovich, A. Fleszar, Verhandlungen der DPG 1 (2001) 66.

<sup>1</sup> The quantities  $E_{\text{SiOSi}}$  and  $E_{\text{SiO}}$  contain information on Pr–Si bonds and therefore should not be confused with the energy of oxygen in a Si dimer bond.